A DIRICHLET–NEUMANN TYPE ALGORITHM FOR CONTACT PROBLEMS WITH FRICTION

ROLF H. KRAUSE* AND BARBARA I. WOHLMUTH†

Abstract. Domain decomposition techniques provide a powerful tool for the numerical approximation of partial differential equations. We introduce a new algorithm for the numerical solution of a nonlinear contact problem with Coulomb friction between linear elastic bodies. The discretization of the nonlinear problem is based on mortar techniques. We use a dual basis Lagrange multiplier space for the coupling of the different bodies. The boundary data transfer at the contact zone is essential for the algorithm. It is realized by a scaled mass matrix which results from the mortar discretization on non-matching triangulations. We apply a nonlinear block Gauß–Seidel method as iterative solver which can be interpreted as a Dirichlet–Neumann algorithm for the nonlinear problem. In each iteration step, we have to solve a linear Neumann problem and a nonlinear Signorini problem. The solution of the Signorini problem is realized in terms of monotone multigrid methods, [Kor97a, Kra01]. Numerical results illustrate the performance of our approach in 2D and 3D.

Key words. mortar finite elements, dual space, Dirichlet–Neumann algorithm, non-matching triangulations, multigrid methods, contact problems, linear elasticity

AMS subject classifications. 65N30, 65N55, 74B10

1. Introduction. We present domain decomposition methods within the framework of mortar techniques [BMP93, BMP94]. Originally introduced as a nonconforming method for the coupling of spectral elements, these techniques can be used in a large class of situations. The coupling of different physical models, discretization schemes or non-matching triangulations along interior interfaces of the domain can be analyzed by mortar methods. These domain decomposition techniques provide a more flexible approach than standard conforming formulations, and are of special interest for time dependent problems, rotating geometries, inhomogeneous materials, problems with local anisotropies, corner singularities, contact problems and when different terms dominate in different regions of the simulation domain. One major requirement to obtain optimal discretization schemes is that the interfaces between the different regions are handled appropriately, see, e.g., [BD98, Ben99, BMP93, BMP94]. Very often, suitable matching conditions at the interfaces can be formulated as weak continuity conditions. Here, we consider mortar finite element formulations based on a dual basis for the Lagrange multiplier space, see [Woh00], with special emphasis on nonlinear contact problems. As a consequence of the biorthogonality relation and in contrast to the standard mortar methods, the locality of the support of the nodal basis functions of the corresponding constrained space is preserved.

We focus on a nonlinear problem modeling the contact of linear elastic bodies. The actual zone of contact is not known in advance and has to be identified during the iteration process. A lot of work has been done on contact problems, see, e.g., [DNS99, WG97, HH80, HH81, ESW99] and [Wri95, IHL88, KO88a] for survey papers. Two main difficulties occur in the numerical simulation of contact problems. The first is the handling of the boundary data transfer at the interface between the two bodies. In our setting, this information transfer is realized in terms of the scaled mass matrix from the mortar formulation. The second difficulty is the intrinsic nonlinearity of the

* Institut für Mathematik I, Freie Universität Berlin, Arnimallee 2, D–14195 Berlin, Germany
Email: krause@math.fu-berlin.de, http://www.math.fu-berlin.de/~krause

†Math. Institut, Universität Augsburg, Universitätsstr. 14, D–86159 Augsburg, Germany.
Email: wohlmuth@math.uni-augsburg.de, http://wwwhoppe.math.uni-augsburg.de/~wohlmuth

problem at the contact boundary. To overcome this difficulty, we use a monotone multigrid method as a subdomain solver, see [Kor97a, KK99, KK00, Kra01]. This method provides an efficient iterative scheme for elliptic obstacle problems including the Signorini problem. We refer to [Kra01] for a theoretical and numerical analyzis. However, it cannot be applied directly to multi body problems with non-matching triangulations. Using mortar techniques for the discretization and a monotone multigrid method as subdomain solver, we introduce a new algorithm for the numerical solution of contact problems. It can be interpreted as a nonlinear Dirichlet–Neumann type preconditioner.

The rest of the paper is organized as follows: In Section 2, we consider a nonlinear contact problem. We focus on the elastic contact without friction between deformable bodies. The discretization at the interface is based on a mortar coupling in terms of a dual Lagrange multiplier space. Using the role of the Lagrange multiplier, we formulate a nonlinear Dirichlet–Neumann algorithm in Section 3. In Section 4, numerical results in 2D are presented illustrating the convergence rates of our algorithm. We extend our approach in Section 5 to contact problems with Coulomb friction. Compared to Section 3, no additional outer iteration is required. Finally in Section 6, numerical results are shown in 2D and 3D illustrating the efficiency and flexibility of our proposed algorithm.

2. A nonlinear frictionless contact problem. In this section, we consider a nonconforming approach for the elastic contact between deformable bodies. One of the major difficulties in the numerical simulation of contact problems is the non-differentiability of the associated energy functional at the contact boundary. Very often regularization techniques; see, e.g., [CSW99, ESW99], or augmented Lagrangian methods; see, e.g., [Tal94, PC99] are used.

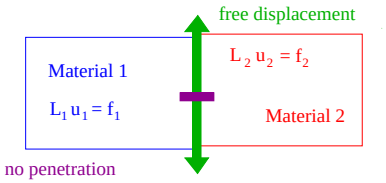

FIG. 2.1. *Nonlinear contact problem*

Figure 2.1 illustrates the situation at the contact zone between two bodies. No penetration between the bodies occurs but free tangential displacement is permitted. For simplicity, we restrict ourselves to the case of two deformable bodies in contact. The two bodies in their reference configuration are identified with the domains $\Omega_k \subset \mathbb{R}^d$, $k = 1, 2$, $d = 2, 3$, and we decompose the solution $\mathbf{u}$ in $\mathbf{u} = (\mathbf{u}_1, \mathbf{u}_2)$, and write $(\mathbf{u}_k)_n := \mathbf{u}_k \cdot \mathbf{n}_k$, $k = 1, 2$, where $\mathbf{n}_k$ is the outer unit normal on $\partial\Omega_k$. The non-mortar side is associated with subdomain Ω_1. We start with the decomposition of the boundary of Ω into three disjoint parts, Γ_D is the Dirichlet part, Γ_N denotes the Neumann part and Γ_C stands for the contact boundary. The actual contact zone between the two bodies is a priori unknown and is assumed to be a subset of Γ_C. We denote tensor and vector quantities by bold symbols, e.g., $\boldsymbol{\tau}$ and $\mathbf{v}$, and its components by τ_{ij} and v_i, $1 \leq i, j \leq d$. The partial derivative with respect to x_j is abbreviated with the index $_{,j}$. Furthermore, we enforce the summation convention on all repeated indices ranging from 1 to d, and we denote by δ_{ij} the Kronecker symbol.

We start with the case that no friction occurs at the contact boundary. Then, the

nonlinear contact problem can be written as a boundary value problem. In addition to the equilibrium conditions in Ω_1 and Ω_2 and the boundary conditions on $\partial\Omega$

$$\begin{array}{rcll} -\sigma_{ij}(\mathbf{u})_{,j} & = & f_i, & \text{in } \Omega_1 \cup \Omega_2 \ , \\ \mathbf{u} & = & 0, & \text{on } \Gamma_D \ , \\ \sigma_{ij}(\mathbf{u}) \cdot n_j & = & p_i, & \text{on } \Gamma_N \ , \end{array} \tag{2.1}$$

we have the following conditions on the possible contact boundary Γ_C

$$\begin{array}{rcccl} \boldsymbol{\sigma}_T(\mathbf{u}_1) & = & \boldsymbol{\sigma}_T(\mathbf{u}_2) & = & 0 \ , \\ \sigma_n(\mathbf{u}_1) & = & \sigma_n(\mathbf{u}_2) & \leq & 0 \ , \end{array} \tag{2.2}$$

and the linearized contact condition on Γ_C

$$\begin{array}{rcl} t & \geq & (\mathbf{u}_1)_n + (\mathbf{u}_2)_n \ , \\ 0 & = & ((\mathbf{u}_1)_n + (\mathbf{u}_2)_n - t)\, \sigma_n(\mathbf{u}_1) \ , \end{array} \tag{2.3}$$

where the function $t\colon \Gamma_C \subset \mathbb{R}^d \longrightarrow \mathbb{R}$ is the distance between the two bodies in normal direction taken with respect to the reference configuration; see [HH80, BGK87]. We assume that t is continuous. The system (2.1) is obtained by the equation of equilibrium, the strain-displacement relation and the constitutive law. In the case of a linear elastic material, the stress tensor $\boldsymbol{\sigma}$ depends linearly on the infinitesimal strain tensor $\boldsymbol{\epsilon}(\mathbf{u}) := 1/2(\nabla\mathbf{u} + \nabla\mathbf{u}^T)$. The stress tensor $\boldsymbol{\sigma}$ is given by Hooke's law

$$\sigma_{ij}(\mathbf{u}) := E_{ijlm}\, u_{l,m} \ ,$$

where Hooke's tensor $\mathbf{E} := (E_{ijlm})_{ijlm=1}^d$, $E_{ijlm} \in L^\infty(\Omega)$, is assumed to be sufficiently smooth, symmetric and uniformly positive definite. In the case of a homogeneous isotropic material, Hooke's tensor has the simple form

$$E_{ijlm} = \frac{E\ \nu}{(1+\nu)(1-2\nu)}\delta_{ij}\delta_{kl} + \frac{E}{2(1+\nu)}(\delta_{ik}\delta_{jl} + \delta_{il}\delta_{jk}) \ ,$$

where $E > 0$ is Young's modulus and $\nu \in (0, 1/2)$ is the Poisson ratio. Figure 2.2 illustrates the normal stress at the contact boundary.

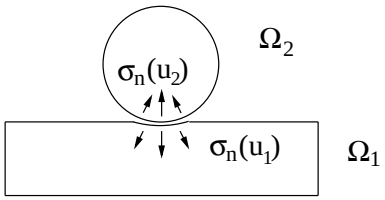

FIG. 2.2. *Normal stress at the contact boundary*

Here, we consider a contact problem without friction. Thus, the tangential component of the stress tensor vanishes at the contact boundary, and is set to zero in the first equation of (2.2). We have only contact pressure at Γ_C. If there is no contact between the two bodies, the boundary stresses at Γ_C are zero; see (2.2) and (2.3). The bilinear form $a(\cdot,\cdot)$ is defined by

$$a(\mathbf{v},\mathbf{w}) := \sum_{k=1}^{2} \int_{\Omega_k} E_{ijlm} w_{i,j} v_{l,m}\, dx, \quad \mathbf{w}, \mathbf{v} \in \prod_{k=1}^{K} \mathbf{H}^1(\Omega_k) \ ,$$

where E_{ijlm} is assumed to be constant on each subdomain and $\mathbf{H}^1(\Omega_k) := (H^1(\Omega_k))^d$. We write $f(\mathbf{v}) := (\mathbf{v}, \mathbf{f})_{0;\Omega} + (\mathbf{v}, \mathbf{p})_{0;\Gamma_N}$ and denote by $f_k(\cdot)$ and $a_k(\cdot,\cdot)$ the restriction of $f(\cdot)$ and $a(\cdot,\cdot)$ to Ω_k , $k = 1, 2$, respectively.

The weak solution of the nonlinear contact problem can be obtained by a minimization problem on a convex set. We define the convex set $\mathcal{K}$ of admissible displacements by

$$\mathcal{K} \;=\; \{\mathbf{v} \in \mathbf{H}^1_*(\Omega_1) \times \mathbf{H}^1_*(\Omega_2) \mid \; (\mathbf{v}_1)_n + (\mathbf{v}_2)_n \leq t\} \;\; ,$$

where $\mathbf{H}^1_*(\Omega_k) \subset \mathbf{H}^1(\Omega_k)$ satisfies homogeneous Dirichlet boundary conditions on $\partial\Omega_k \cap \Gamma_D$. Then, the weak solution of (2.1)–(2.3) is defined by: Find $\mathbf{u} \in \mathcal{K}$ such that

$$J(\mathbf{u}) \;\leq\; \min_{\mathbf{v}\in\mathcal{K}} J(\mathbf{v}) \;\; , \tag{2.4}$$

where the energy functional $J(\cdot)$ is given by $J(\mathbf{v}) := \frac{1}{2}a(\mathbf{v},\mathbf{v}) - f(\mathbf{v})$ on $\mathcal{K}$; see, e.g., [HH80, BGK87]. The minimization problem (2.4) is equivalent to a variational inequality: Find $\mathbf{u} \in \mathcal{K}$ such that

$$a(\mathbf{u}, \mathbf{v}-\mathbf{u}) \;\geq\; f(\mathbf{v}-\mathbf{u}), \qquad \mathbf{v} \in \mathcal{K} \;\; .$$

Our approach on the discrete level is based on a Neumann–Dirichlet algorithm and inexact solvers. In each step, a linear inhomogeneous Neumann problem has to be solved. This is done by standard multigrid techniques. Furthermore, a nonlinear one-sided contact problem has to be solved. Here, we use monotone multigrid methods; see [Kor97b, KK00, Kra01]. The information transfer at the contact boundary is realized in terms of the scaled mass matrix. The major advantages of this new approach are the efficiency of the iterative solver, and the a priori estimates for the boundary stresses at the actual contact zone. Introducing the boundary stress formally as Lagrange multiplier, the Neumann–Dirichlet formulation can be interpreted as a mortar setting. In contrast to penalty methods, the discretization error of the boundary stresses does not depend on regularization parameters.

To motivate our approach, let us assume for the moment that the contact stress σ_n is known on Γ_C. Then, problem (2.1)–(2.3) can be decoupled in the following way: In a first step, we solve an inhomogeneous Neumann problem on Ω_2: Find $\mathbf{u}_2 \in \mathbf{H}^1_*(\Omega_2)$ such that

$$a_2(\mathbf{u}_2, \mathbf{v}) = f_2(\mathbf{v}) + (\sigma_n, \mathbf{v}_n)_{0;\Gamma_C}, \qquad \mathbf{v} \in \mathbf{H}^1_*(\Omega_2) \;\; . \tag{2.5}$$

Having $\mathbf{u}_2 \in \mathbf{H}^1_*(\Omega_2)$, $\mathbf{u}_1 \in \mathbf{H}^1_*(\Omega_1)$ can be obtained in terms of $\mathbf{u}_2|_{\Gamma_C}$. We define the convex set $\mathcal{K}_{\mathbf{v}_2}$ of admissible displacements for a given $\mathbf{v}_2 \in \mathbf{H}^1_*(\Omega_2)$

$$\mathcal{K}_{\mathbf{v}_2} \;:=\; \{\mathbf{v}_1 \in \mathbf{H}^1_*(\Omega_1) \mid (\mathbf{v}_1)_n \leq t - (\mathbf{v}_2)_n \text{ on } \Gamma_C\} \;\; .$$

Then, the one-sided contact problem on Ω_1 can be written as a variational inequality: Find $\mathbf{u}_1 \in \mathcal{K}_{\mathbf{u}_2}$ such that

$$a_1(\mathbf{u}_1, \mathbf{v}-\mathbf{u}_1) \;\geq\; f_1(\mathbf{v}-\mathbf{u}_1), \qquad \mathbf{v} \in \mathcal{K}_{\mathbf{u}_2} \;\; . \tag{2.6}$$

The discretization of the set $\mathcal{K}_{\mathbf{v}_2}$ is given by

$$\mathcal{K}^h_{\mathbf{v}_2} \;:=\; \{\mathbf{v}_1 \in \mathbf{X}_{1,h} \mid (\mathbf{v}_1)_n(p) \leq t(p) - (\Pi\mathbf{v}_2)_n(p) \text{ for all } p \in \mathcal{P}_C\} \;\; , \tag{2.7}$$

where $\mathbf{X}_{k,h}$ is the finite element space $\mathbf{X}_h \cap \mathbf{H}^1_*(\Omega_k)$, $k = 1, 2$, of vector valued piecewise linear hat functions on Ω_k. $\mathcal{P}_C$ denotes the set of vertices on the non-mortar side of $\overline{\Gamma}_C$, and Π is a suitable mapping from the mortar side on the non-mortar side. In the conforming case where $\Pi = \mathrm{Id}$ is the standard choice, a priori estimates for the discretization error can be found in, e.g., [KO88b]. We refer to [BHL97, BHL99] for an a priori analysis in the nonconforming case. Results on a posteriori error estimation for unilateral contact problems can be found in [CHP00]. Numerical examples for a mortar coupling with standard Lagrange multipliers in 2D without friction are given in [Hil00]. In the following, we do not use an additional index h to denote the discrete approximation $\mathbf{u} = (\mathbf{u}_1, \mathbf{u}_2) \in \mathbf{X}_{1,h} \times \mathbf{X}_{2,h}$, and $\boldsymbol{\lambda}$ stands for the discrete boundary stress. Here, in an abuse of notation, we do not distinguish between an element $\mathbf{v} \in \mathbf{X}_h$ and its vector representation with respect to the standard nodal basis. In addition, we identify the spaces $\mathbf{X}_{k,h}$ and $\mathbb{R}^{n_k}$, $n_k := \dim \mathbf{X}_{k,h}$, $k = 1, 2$. For $k = 1, 2$, we denote by A^k_N the stiffness matrix with respect to $a_k(\cdot, \cdot)$ and by $\mathbf{f}_k$ the vector associated with the right hand side. The index N of A^k_N indicates that the stiffness matrix corresponds to Neumann type boundary conditions at the interface.

Before we formulate our algorithm, we consider the information transfer at the interface in more detail. We define the projection Π in terms of a dual Lagrange multiplier space. Let ϕ_j, $1 \le j \le N_C$, be the standard piecewise linear hat functions associated with the non-mortar side. $N_C := \#\mathcal{P}_C$ stands for the number of vertices on the non-mortar side. We denote by ψ_j, $1 \le j \le N_C$, a set of locally defined piecewise linear biorthonormal basis functions, i.e.,

$$\int_{\Gamma_C} \psi_j \phi_l \, ds = \delta_{jl}, \quad 1 \le j, l \le N_C \ .$$

Moreover, we assume that $P_0(\Gamma_C) \subset \mathrm{span}\,\{\psi_j, 1 \le j \le N_C\} =: M_h$. The existence of such basis functions supported by two edges has been established, see, e.g., [Woh01]. We note that in contrast to a standard mortar approach with crosspoints, no modification of the dual basis functions in the neighborhood of the endpoints of Γ_C is necessary. Now, we define our projection $\Pi \colon \mathbf{X}_{2,h} \longrightarrow \mathbf{X}_{1,h}$,

$$(\Pi\ \mathbf{v})_i := \sum_{j=1}^{N_C} \int_{\Gamma_C} v_i\ \psi_j\ ds\ \ \phi_j\,, \quad \mathbf{v} \in \mathbf{X}_{2,h}\,, \quad 1 \le i \le d \ .$$

It is clear that Π can also be applied to $\mathbf{v}_2 \in \mathbf{H}^1_*(\Omega_2)$. We denote the algebraic representation of Π as function from $\mathbb{R}^{n_2}$ onto $\mathbb{R}^{n_1}$ by S, and we observe that S is a $n_1 \times n_2$ matrix, which consists of large zero blocks and one non zero block associated with the vertices on the non-mortar and mortar side. Solving a discrete Dirichlet problem on Ω_1 provides an approximation for the corresponding flux $\boldsymbol{\lambda} \in \mathbf{M}_h := (M_h)^d$ on Γ_C. Within the mortar approach the discrete flux $\boldsymbol{\lambda}$ is uniquely defined by

$$\int_{\Gamma_C} \boldsymbol{\lambda}\ \mathbf{v}\, ds = a_1(\mathbf{u}_1, \mathbf{v}) - f_1(\mathbf{v}), \quad \mathbf{v} \in \mathbf{X}_{1,h} \ .$$

Using $\boldsymbol{\lambda} \in \mathbf{M}_h$ in (2.5), we find for an element $\mathbf{v}_2$ in $\mathbf{X}_{2,h}$

$$\int_{\Gamma_C} \boldsymbol{\lambda}\ \mathbf{v}_2\, ds = \int_{\Gamma_C} \boldsymbol{\lambda}\ \Pi \mathbf{v}_2\, ds = \int_{\Gamma_C} \Pi^* \boldsymbol{\lambda}\ \mathbf{v}_2\, ds \ ,$$

where Π^* denotes the adjoint operator of Π. The matrix representation of which is given by S^T. Here, we identify $\mathbf{M}_h$ with $\mathbb{R}^m$, $m := \dim\, \mathbf{M}_h \le n_1$, and use the

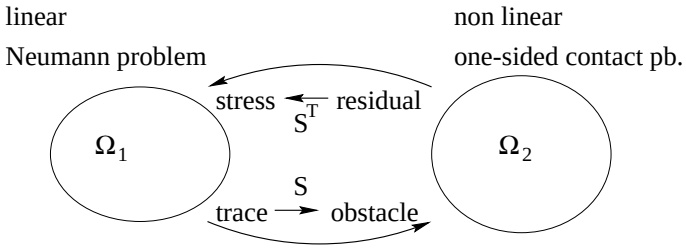

FIG. 2.3. *Discrete Dirichlet–Neumann coupling*

embedding $\mathbb{R}^m \subset \mathbb{R}^{n_1}$. Figure 2.3 illustrates the role of discrete transfer operators S and S^T.

The transfer of the Dirichlet values at the contact boundary is realized in terms of the linear operator Π and the transfer of the boundary stresses in terms of the adjoint operator, corresponding to the duality between displacements and stresses. In the algebraic formulation, the matrix S is used to transfer the displacements on the mortar side as Dirichlet values, or more precisely as an obstacle, onto the non-mortar side, and the scaled boundary stresses are transferred from the non-mortar side to the mortar side in terms of the transposed matrix S^T. The interface conditions of the mortar formulation guarantee that (2.2) and (2.3) are satisfied in a weak integral form.

3. Dirichlet–Neumann algorithm. Now, our nonlinear Neumann–Dirichlet algorithm is defined in terms of $\mathbf{f}_1$, $\mathbf{f}_2$ and S:

Choose damping parameters: $0 < \omega_D, \omega_N \leq 1$.

Initialize: $\mathbf{X}_{1,h} \ni \mathbf{g}^0 = 0,\ \mathbf{X}_{2,h} \ni \mathbf{p}^1 = 0$.

For $\mu = 1, \ldots, N$ *do*

Solve linear Neumann problem: Find $\mathbf{u}_2^\mu \in \mathbf{X}_{2,h}$*:*

$$A_N^2 \mathbf{u}_2^\mu = \mathbf{f}_2 - \mathbf{p}^\mu \ .$$

Transfer of the displacement and damping:

$$\mathbf{g}^\mu = (1 - \omega_D)\mathbf{g}^{\mu-1} + \omega_D S \mathbf{u}_2^\mu \ .$$

Solve nonlinear one-sided contact problem: Find $\mathbf{u}_1^\mu \in \mathcal{K}^h_{\mathbf{g}^\mu}$*:*

$$(A_N^1 \mathbf{u}_1^\mu, \mathbf{v} - \mathbf{u}_1^\mu) \geq (\mathbf{f}_1, \mathbf{v} - \mathbf{u}_1^\mu), \qquad \mathbf{v} \in \mathcal{K}^h_{\mathbf{g}_n^\mu} \ .$$

Compute the residual $\mathbf{r}_1^\mu \in \mathbf{X}_{1,h}$*:*

$$\mathbf{r}_1^\mu = A_N^1 \mathbf{u}_1^\mu - \mathbf{f}_1 \ .$$

Transfer of the boundary stress and damping:

$$\mathbf{p}^{\mu+1} = (1 - \omega_N)\mathbf{p}^\mu + \omega_N S^T \mathbf{r}_1^\mu \ .$$

In each step of our algorithm, we use a multigrid methods as solver. The variational inequality can be solved efficiently by monotone multigrid methods. The main idea is to minimize the energy functional $J_1(\cdot)$ on $\mathcal{K}^h_{\mathbf{u}_2}$ successively in direction of appropriate

test functions. Choosing the multilevel nodal basis of a multigrid hierarchy as test functions, this turns out to be a combination of a projected block Gauß–Seidel on the finest grid with locally damped coarse grid corrections, and can be implemented as a modified $\mathcal{V}$-cycle. Since the coarse grid corrections have to satisfy the constraints given by (2.7) with respect to the finest triangulation, suitable non-trivial coarse grid functions have to be constructed. The construction of the modified coarse grid corrections can be found in [Kra01]. It can be shown, that after a finite number of iterations the discrete contact boundary is identified; see [Kor97a]. Then, the method degenerates to a standard multigrid method with special treatment of the eventually curvilinear contact boundary. For details and a convergence theory, we refer to [KK99, KK00, Kra01].

Figure 3.1 illustrates the steps of our Neumann–Dirichlet algorithm for $\omega_D = 1$. On the left, the first step is shown. The choice $\mathbf{p}^1 = 0$ implies that a homogeneous Neumann problem has to be solved for $\mathbf{u}_2^1$. In the case that we have a full symmetric problem, it can be easily seen that the choice $\omega_N = 1$ does not yield a convergent scheme. The iterates oscillate between the two first iterates, i.e., $\mathbf{u}_2^{2m+1} = \mathbf{u}_2^1$, $\mathbf{u}_2^{2m+2} = \mathbf{u}_2^2$, $m \geq 1$.

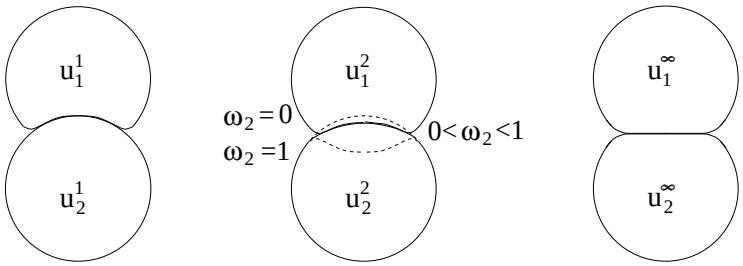

FIG. 3.1. *First iterates* $(\mathbf{u}_1^1, \mathbf{u}_2^1)$ *(left), second iterates (middle) and solution (right)*

REMARK 3.1. *If the actual contact zone is known, problem (2.1)–(2.3) will be linear. In this case, we can expect the same order of convergence as for a standard Neumann–Dirichlet type preconditioner for mortars, see [Dry99, Dry01].*

In the mortar setting, the Lagrange multiplier plays the role of Neumann boundary conditions. The combination of mortar finite elements, monotone multigrid methods and domain decomposition techniques defines in a natural way a new solution algorithm for elastic contact problems. The discrete boundary stress in the μ-th iteration step $\boldsymbol{\lambda}^\mu$ is the residual $\mathbf{r}_1^\mu$ restricted on Γ_C., Moreover, we obtain the normal stress σ_n and the tangential stress σ_T by a local rotation from the final $\boldsymbol{\lambda}^\mu$. We remark, that our approach satisfies $\sigma_T = 0$, although we do not enforce this condition on the discrete space $\mathbf{M}_h$.

REMARK 3.2. *Using the vector valued approach for the Lagrange multiplier space, friction terms can be easily included. The first equation in (2.2) has to be replaced by some friction law, e.g., the Coulomb friction.*

For frictionless contact, the first equation in (2.2) can also be satisfied in its strong form. Then, the Lagrange multiplier space is a scalar function and the mortar approach has to be modified. In particular at the contact boundary, we have to impose Neumann type boundary conditions in tangential direction and an obstacle in normal direction.

4. Numerical results. Finally, we present numerical examples for the proposed algorithm. All our numerical results are carried out within the framework of the finite element toolbox UG, [BBJ+97]. Our first test problem is the Hertzian contact of a linear elastic circle with a linear elastic plane. In this example, the contact stresses can be computed analytically [Her82]. To test the performance of our algorithm, we compare the computed boundary stresses with the analytical ones. For comparability, we choose the same problem data and geometry as in [CSW99]. We consider an elastic circle with scaled material parameters $E = 7000$, $\nu = 0.3$ and radius $r = 1$, pressed by a point load $F = 100$ to a plane with material parameters $E = 10^6$, $\nu = 0.45$.

As is done in [CSW99], we apply the single load as surface load to avoid a singularity. We use bilinear functions on quadrilaterals. Figure 4.1 illustrates the performance of our method. In the left, the maximal contact stress on each level is given, in the middle the contact stresses and tangential stresses are shown, and in the right, the component $\sigma_{22}(\mathbf{u})$ of the stress tensor is depicted. The analytical value of $\sigma_n^{\max} = 495$ is already reached on level 5. Here, only 5 nodes of the circle are actual in contact with the plane. To demonstrate the flexibility of our approach, we do not enforce $\boldsymbol{\sigma}_T = 0$ on the space. The Lagrange multiplier of the mortar method plays the role of the boundary stresses at Γ_C. Thus, the boundary stresses are handled as additional unknowns which are obtained by restricting the residual. This observation predestinates our algorithm for contact problems with friction.

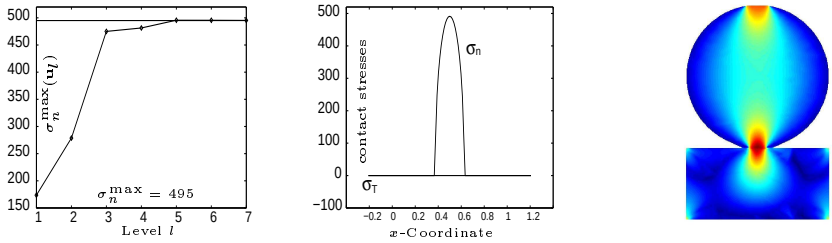

FIG. 4.1. *Maximal contact stresses (left), contact stresses (middle) and σ_{22} (right)*

As long as the discrete contact boundary is not fully recognized, the convergence of the monotone multigrid method might be slow. This is due to the search for the contact boundary. In this example, the contact boundary is detected after at most three inner iterations, i.e., three iterations of the monotone multigrid method, and no slowdown occurs.

We define the stopping criteria for our iterative solver in terms of the Lagrange multiplier. Observing that the choice of our start vectors guarantees $A_N^1 \mathbf{u}_1^n - \mathbf{f}_1 = 0$ for all interior nodes on Ω_1, we find $\|(A_N^1 \mathbf{u}_1^n - \mathbf{f}_1)_{\Gamma_C}\| = \|A_N^1 \mathbf{u}_1^n - \mathbf{f}_1\|$. Moreover $\mathbf{p}^\mu$ can be interpreted as boundary stress on the mortar side in the μ-th iteration step. This observation motivates our stopping criteria

$$\frac{\|\mathbf{p}^{\mu+1} - \mathbf{p}^\mu\|}{\|\mathbf{p}^\mu\|} \leq \mathrm{TOL} \frac{\|\mathbf{p}^3 - \mathbf{p}^2\|}{\|\mathbf{p}^2\|} \tag{4.1}$$

which is equivalent to $\|\mathbf{p}^\mu - S^T \mathbf{r}_1^\mu\| / \|\mathbf{p}^\mu\| \leq \mathrm{TOL} \|\mathbf{p}^2 - S^T \mathbf{r}_1^2\| / \|\mathbf{p}^2\|$. The use of the Euclidean vector norm is motivated by the mesh dependent norm $h\|\cdot\|^2_{0;\Gamma_C}$ for the Lagrange multiplier. We note that if the discrete boundary stress $\mathbf{p}$ is equal zero, then the contact problem is degenerated and two linear problems on Ω_1 and Ω_2 with homogeneous Neumann boundary conditions on Γ_C have to be solved. In that case

since $\mathbf{p}^1 = 0$, $\mathbf{g}^0 = 0$, we obtain the solution after one step. Moreover if $\mathbf{p} \neq 0$, $\omega_D = 1$ and $\mathbf{p}^{\mu_0} = 0$, $\mu_0 \geq 2$, the algorithm does not convergence and the damping parameter ω_N is too large. Table 4.1 shows the number of required iteration steps depending on the damping parameter and the refinement level. We set TOL $= 10^{-4}$. If the damping parameters are small enough the number of required iteration steps can be bounded independently of the refinement level. Here we use uniform refinement on all levels. We observe a considerably smaller number of required iteration steps on Level 2 and Level 3 for $\omega_D = 1$ and $\omega_N = 0.4, 0.5$; see also Figure 4.3.

TABLE 4.1
Number of iteration steps, (Lagrange multiplier norm)

	lev. 0	lev. 1	lev. 2	lev. 3	lev. 4	lev. 5	lev. 6
$\omega_D = 1$, $\omega_N = 0.5$	11	11	5	6	13	10	12
$\omega_D = 1$, $\omega_N = 0.4$	14	14	8	9	18	15	16
$\omega_D = 0.5$, $\omega_N = 1$	12	11	6	6	6	8	11
$\omega_D = 0.4$, $\omega_N = 1$	16	16	9	10	8	11	11
$\omega_D = 0.6$, $\omega_N = 0.8$	9	8	8	9	7	8	9
$\omega_D = 0.8$, $\omega_N = 0.6$	6	7	9	9	10	8	9
$\omega_D = 0.7$, $\omega_N = 0.7$	8	7	10	9	9	8	9

Figure 4.2 illustrates the influence of the choice of the damping parameters. The error reduction $g(\mu) := \|\mathbf{p}^{\mu+2} - S^T\mathbf{r}_1^{\mu+2}\| \, \|\mathbf{p}^2\| / \|\mathbf{p}^{\mu+2}\| \, \|\mathbf{p}^2 - S^T\mathbf{r}_1^2\|$ is shown versus the number μ of iteration steps. If the damping parameter is small enough level independent upper bounds for the convergence rates can be observed.

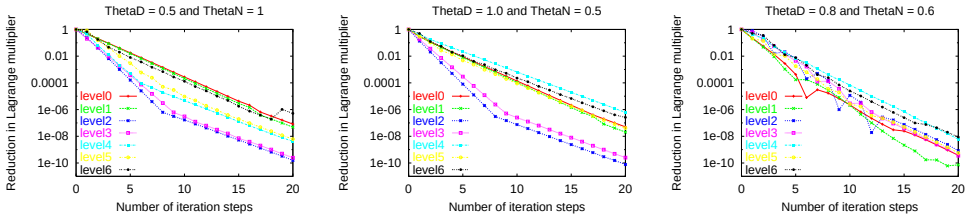

FIG. 4.2. *Error reduction for different damping parameters ω_N, ω_D*

Figure 4.3 illustrates the influence of small and too large damping factors. Small damping parameters lead to a slow convergence, see the left and middle picture in Figure 4.3. On the other hand, the algorithm does not converge for higher levels if the damping parameter is too large, see the right picture in Figure 4.3.

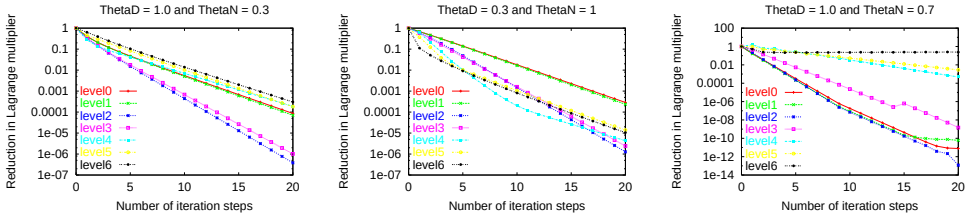

FIG. 4.3. *Influence of too small and too large damping parameters*

To be on the safe side, one has to chose a small damping factor. Unfortunately, the optimal damping parameter is in general not known. Adaptive strategies controlling the damping parameter might yield considerably better results. A different possibility to improve the performance is the use of our algorithm as preconditioner for a Krylov subspace method. As soon as the actual zone of contact is detected, we are in the linear setting. Then, our algorithm for $\omega_D = 1$ is equivalent to a preconditioned Schur complement system, and we can apply a conjugate gradient method.

In our next example, we consider the elastic contact of a wrench and a nut. At the interior boundary of the nut, i.e., the part of the boundary with outer normal pointing towards the center of gravity of the nut, we impose Dirichlet boundary conditions corresponding to a rotation. Homogeneous Dirichlet boundary conditions are applied at the handle of the wrench and on all remaining parts of the boundary we impose homogeneous Neumann conditions. We use linear elements on triangles, and refinement is done adaptively. As can be seen in the right of Figure 4.4, the actual contact zone is only a small part of the contact boundary Γ_C. We remark, that a more realistic model would include friction at the interface.

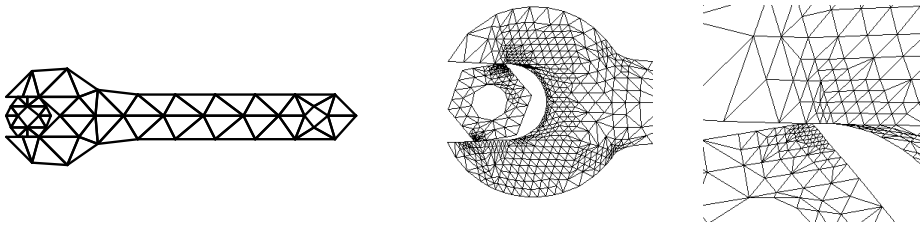

FIG. 4.4. *Initial triangulation (left), deformation and final triangulation (middle) and zoom at the contact zone (right)*

5. A contact problem with Coulomb friction. In this section, we consider a nonlinear contact problem with friction. For simplicity we restrict ourselves to the classical Coulomb friction, and we do not consider more general non local friction laws; see [KO88b]. Let us consider for the moment the Signorini problem where an elastic body is in contact with a rigid foundation. In that situation, the Coulomb law can be described as follows: As long as the norm of the tangential stress is small enough, no sliding occurs, and the tangential displacement is zero. If the norm of the tangential stress $\boldsymbol{\sigma}_T$ reaches a critical limit, which is proportional to the absolute values of the normal stress, sliding in the opposite direction of $\boldsymbol{\sigma}_T$ can be observed; see [KO88b]. Figure 5.1 illustrates the relation between tangential stress and normal stress for a sliding and a sticky node.

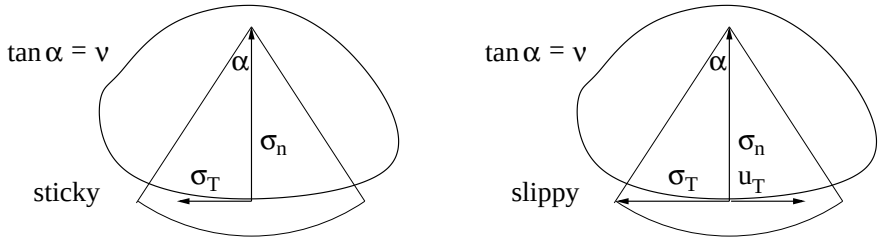

FIG. 5.1. *Sticky node (left) and sliding node (right)*

The Coulomb law can be applied for two linear elastic bodies in contact if we replace the tangential displacement by the relative tangential displacement; see [IW92, Eck96]. Then, the equilibrium conditions at the contact boundary and the Coulomb's law read as follows:

$$\begin{array}{ll} \boldsymbol{\sigma}_T(\mathbf{u}_1) = \boldsymbol{\sigma}_T(\mathbf{u}_2), & \sigma_n(\mathbf{u}_1) = \sigma_n(\mathbf{u}_2) \le 0 \ , \\ |\boldsymbol{\sigma}_T(\mathbf{u}_1)| \le \nu|\sigma_n(\mathbf{u}_1)|, & \boldsymbol{\sigma}_T(\mathbf{u}_1)[\mathbf{u}_T] + \nu|\sigma_n(\mathbf{u}_1)|\,|[\mathbf{u}_T]| = 0 \ , \end{array} \tag{5.1}$$

where $\nu > 0$ is the friction coefficient and the jump is defined by $[\mathbf{u}_T] := (\mathbf{u}_1)_T - (\mathbf{u}_2)_T$. An equivalent formulation of Coulomb's law can be given by $|\boldsymbol{\sigma}_T(\mathbf{u}_1)| \le \nu|\sigma_n(\mathbf{u}_1)|$ and

$$\begin{array}{llll} \text{if} & |\boldsymbol{\sigma}_T(\mathbf{u}_1)| < \nu|\sigma_n(\mathbf{u}_1)| & \Longrightarrow & [\mathbf{u}_T] = 0 \\ \text{if} & |\boldsymbol{\sigma}_T(\mathbf{u}_1)| = \nu|\sigma_n(\mathbf{u}_1)| & \Longrightarrow & [\mathbf{u}_T] = -s\boldsymbol{\sigma}_T(\mathbf{u}_1), \quad s \ge 0 \ ; \end{array}$$

see also [Has92, KB92]. Then, the equilibrium condition satisfies the boundary value problem given by (2.1), (2.3) and (5.1). As in the frictionless case, we base our numerical approach on the variational formulation. To do so, we use the principle of virtual work and introduce a nonlinear functional $j(\cdot,\cdot)$ to describe the virtual work of the frictional force

$$j(\mathbf{u},\mathbf{v}) := \int_{\Gamma_C} \nu|\sigma_n(\mathbf{u}_1)|\,|[\mathbf{v}_T]|\,ds \ .$$

Following the lines of [KO88b, Chapter 10], a variational inequality can be obtained from (2.1), (2.3) and (5.1) by applying Green's formula. The weak form of (2.1), (2.3) and (5.1) reads as follows: Find $\mathbf{u} \in \mathcal{K}$ such that

$$a(\mathbf{u}, \mathbf{v}-\mathbf{u}) + j(\mathbf{u},\mathbf{v}) - j(\mathbf{u},\mathbf{u}) \ge f(\mathbf{v}-\mathbf{u}), \quad \mathbf{u} \in \mathcal{K} \ . \tag{5.2}$$

Moreover under suitable assumptions on the data, (5.2) and (2.1), (2.3) and (5.1) are equivalent; see [Eck96, Satz 1.6]. We do not address questions such as existence, uniqueness and regularity of a solution. Recently existence results for a large class of contact problems with friction have been obtained. We refer to [Eck96, EJ98, IHL88, NJH80] and the references therein. Very often existence proofs are based on penalization and regularization techniques, and bounds for the admissible friction coefficient can be established; see [EJ98].

We follow, the lines of the previous paragraph to motivate our algorithm. Let us assume that the boundary stresses $\boldsymbol{\sigma}_T$ and σ_n are known on the contact boundary. Then, the boundary value problem (2.1), (2.3) and (5.1) can be decoupled. The solution on ω_N can be obtained as the solution of an inhomogeneous Neumann problem: Find $\mathbf{u}_2 \in \mathbf{H}^1_*(\omega_N)$ such that

$$a_2(\mathbf{u}_2,\mathbf{v}) = f_2(\mathbf{v}) + (\sigma_n, \mathbf{v}_n)_{0;\Gamma_C}, + (\boldsymbol{\sigma}_T, \mathbf{v}_T)_{0;\Gamma_C} \qquad \mathbf{v} \in \mathbf{H}^1_*(\omega_N) \ .$$

To obtain $\mathbf{u}_1$, we solve a nonlinear one-sided contact problem with Coulomb friction on Ω_1. Then, the variational inequality (5.2) reduces to $\mathbf{u}_1 \in \mathcal{K}_{\mathbf{u}_2}$

$$a_1(\mathbf{u}_1, \mathbf{v}-\mathbf{u}_1) + j^{\mathrm{red}}_{\sigma_n;\mathbf{u}_2}(\mathbf{v}) - j^{\mathrm{red}}_{\sigma_n;\mathbf{u}_2}(\mathbf{u}_1) \ge f_1(\mathbf{v}-\mathbf{u}_1), \quad \mathbf{v} \in \mathcal{K}_{\mathbf{u}_2} \ ,$$

where the reduced form of the virtual work for a given function s and a given displacement $\mathbf{w}$ is defined by

$$j^{\mathrm{red}}_{s,\mathbf{w}}(\mathbf{v}) := \int_{\Gamma_C} \nu\,|s|\,|\mathbf{v}_T - \mathbf{w}_T|\,ds \ . \tag{5.3}$$

This type of friction law where the contact stress is assumed to be known is also called Tresca friction. Now, we proceed as in the previous paragraph and carry out a fixed point iteration. Our nonlinear Neumann–Dirichlet algorithm for a contact problem with Coulomb friction reads as:

Choose damping parameters: $0 < \omega_D, \omega_N \leq 1$.
Initialize: $\mathbf{X}_{1,h} \ni \mathbf{g}^0 := 0,\ \mathbf{X}_{2,h} \ni \mathbf{p}^1 := 0$.
For $\mu = 1, \ldots, N$ *do*

Solve linear Neumann problem: Find $\mathbf{u}_2^\mu \in \mathbf{X}_{2,h}$*:*

$$A_N^2 \mathbf{u}_2^\mu = \mathbf{f}_2 - \mathbf{p}^\mu \ .$$

Transfer of displacements and damping:

$$\mathbf{g}^\mu = (1 - \omega_D)\mathbf{g}^{\mu-1} + \omega_D S \mathbf{u}_2^\mu \ .$$

Solve nonlinear one-sided contact problem with Coulomb friction:
Find $\mathbf{u}_1^\mu \in \mathcal{K}^h_{\mathbf{g}^\mu}$*:*

$$(A_N^1 \mathbf{u}_1^\mu, \mathbf{v} - \mathbf{u}_1^\mu) + \mathbf{j}^{\mathrm{red}}_{(\mathbf{r}_1^\mu)_n;\mathbf{g}^\mu}(\mathbf{v}) - \mathbf{j}^{\mathrm{red}}_{(\mathbf{r}_1^\mu)_n;\mathbf{g}^\mu}(\mathbf{u}_1^\mu) \geq (\mathbf{f}_1, \mathbf{v} - \mathbf{u}_1^\mu), \quad \mathbf{v} \in \mathcal{K}^h_{g_n^\mu} \ .$$

Compute the residual $\mathbf{r}_1^\mu \in \mathbf{X}_{1,h}$*:*

$$\mathbf{r}_1^\mu = A_N^1 \mathbf{u}_1^\mu - \mathbf{f}_1 \ .$$

Transfer of scaled boundary stresses and damping:

$$\mathbf{p}^{\mu+1} = (1 - \omega_N)\mathbf{p}^\mu + \omega_N S^T \mathbf{r}_1^\mu \ .$$

Here, $\mathbf{j}^{\mathrm{red}}_{\cdot;\cdot}(\cdot)$ is the algebraic representation of the nonlinear functional $j^{\mathrm{red}}_{\cdot;\cdot}(\cdot)$ defined by (5.3). A possible approach for the analysis of our fixed point iteration is the theory of quasi-variational inequalities, i.e., such inequalities where the convex set depends on the solution; see [GJT81, BC84]. The iterative solution of the nonlinear subproblem is discussed and analyzed in [Kra01].

6. Numerical results with Coulomb friction. In this section, we present some numerical results in 2D and 3D illustrating the influence of the Coulomb friction on the deformation. In all our 2D results, the friction coefficient is $\nu = 0.3$. We start with the Hertz problem of Section 4. Figure 6.1 shows the boundary stresses at the contact zone. The initial triangulation has four elements on each subdomain.

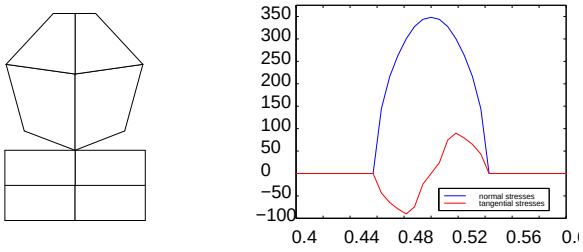

FIG. 6.1. *Initial triangulation (left) and boundary stresses (right)*

Comparing Figure 6.1 with Figure 4.1, we find that the actual zone of contact

and the maximal normal stress are considerably smaller if Coulomb friction occurs. Between the minimum and the maximum of the tangential stress no sliding occurs at the contact zone. Sliding nodes can be found in the neighborhood of the left and right endpoints of the actual contact.

As a second example in 2D we consider a symmetric problem. Here due to the symmetry, we expect that the tangential stress is zero even if friction terms are included. Figure 6.2 shows the boundary stress for the frictionless case and for the case including Coulomb friction. Comparing the left and right picture in Figure 6.2, we find exactly the same values for the normal stress and thus the actual zone of contact.

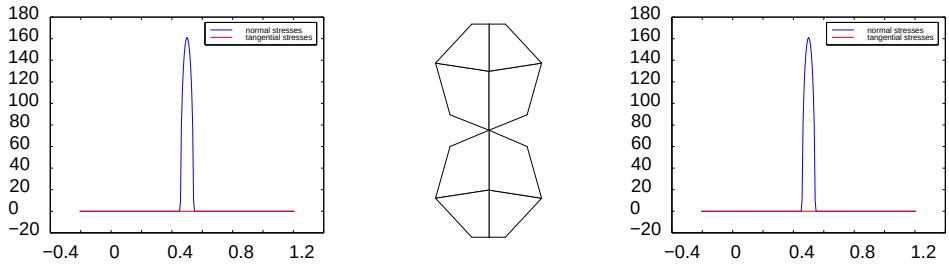

FIG. 6.2. *Boundary stresses (frictionless) (left), initial triangulation (middle) and boundary stresses (Coulomb friction) (right)*

In contrast to the unsymmetric problem in Figure 6.1, no tangential stress occurs. Since the normal and tangential stress is the same at Γ_C, the discrete solutions for the two situations are the same. Figure 6.3 illustrates the stress component σ_{22} close to the contact zone. Although our Dirichlet Neumann algorithm is non symmetric, we obtain a symmetric numerical approximation. The numerical results confirms the flexibility and reliability of the non-conforming approach in terms of dual Lagrange multipliers.

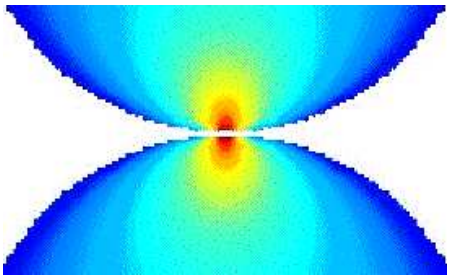

FIG. 6.3. *Boundary stress* σ_{22}

In our last example, we consider the elastic contact of three bodies in 3D. Two cylinders are in contact with a hexahedral bar. At the top and bottom of the upper and lower cylinder, respectively, a displacement in vertical direction towards the bar is enforced. As before in 2D, we start with a very coarse initial triangulation, see Figure 6.4. On Level 0, we only have 5 elements. We use a standard mean value adaptive refinement strategy. The local refinement is controlled by a residual based local a posteriori error indicator on the subdomains and the information transfer at the interface is realized by additional terms in the definition of the local error indicator. On the non-mortar side of the actual contact zone, the local jump $1/h\|[\mathbf{u}]\|^2_{0;\Gamma_C}$ measures the non-conformity which controls the discrete non-penetration condition.

On the mortar side, we add locally the term $h\|[\boldsymbol{\lambda}]\|^2_{0;\Gamma_C}$ which controls the discrete equilibrium condition for the stress at the contact boundary. Here, we interprete λ as a discrete approximation of the stress. In the mortar context, the algebraic relation between the values on mortar λ_m and non-mortar λ_{nm} side are given by

$$\lambda_m = S^T \lambda_{nm},$$

where λ_m and λ_{nm} are set to zero in the interior of the subdomains. We note that we have used discontinuous dual basis functions on both sides of the contact zone to approximate the stress.

The local weights $1/h$ and h reflect the duality between the $H^{1/2}$ and $H^{-1/2}$ spaces. In contrast to conforming methods, no refinement rules have to be considered at the interfaces.

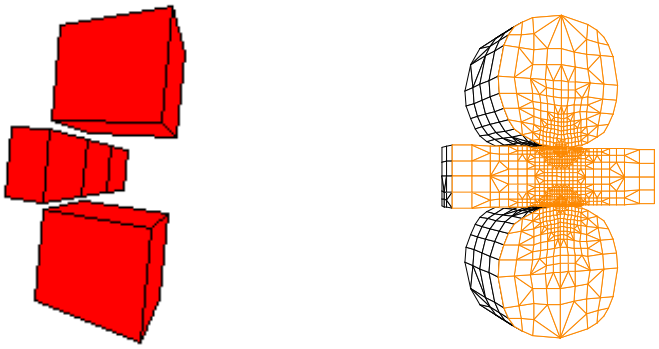

FIG. 6.4. *Initial (left) and adaptive (right) triangulation of a three body contact problem in 3D*

In the right picture in Figure 6.4 a cut of the adaptive triangulation on Level 7 is depicted, showing the meshes in the interior of the computational domain. We observe strong refinement in the neighborhood of the contact zone. Instead of $10,485,760$ elements in the case of uniform refinement, we have $207,561$ elements on Level 7. Using a coefficient of friction of $\nu = 0.25$, we obtain 210 non-mortar nodes in contact on the finest level and 186 sticky nodes. We note, that no element at the interface has been refined within the last refinement step.

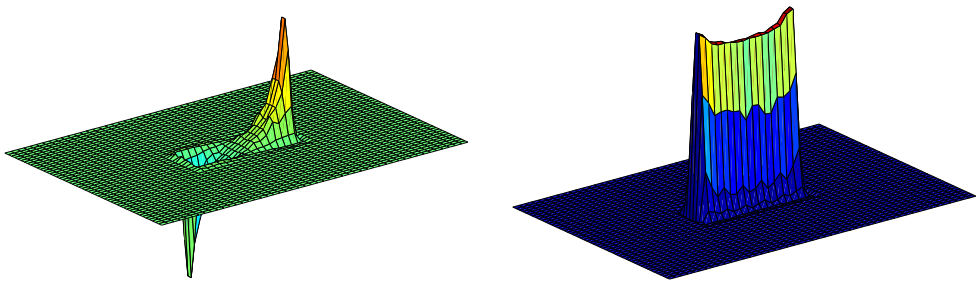

FIG. 6.5. *Tangential (left) and normal (right) stress at one of the interfaces*

The asymptotic convergence rate of our algorithm depends highly on the aspect ratio of the hexahedral bar. It can be improved by using the proposed algorithm

as a preconditioner within a Krylov subspace method. Finally, Figure 6.5 shows the coefficients with respect to the dual basis of the stress in normal direction and of one stress component in tangential direction. The second tangential component is of smaller size. The contact stresses are depicted with respect to the surface of the upper cylinder. This choice is arbitrary, since the problem is symmetric with respect to the symmetry plane of the two cylinders. Since the width of the cylinder in direction of the axis of the cylinder is larger than the width of the bar, the normal stress is zero at the part of the cylinder's surface being on the left and right of the bar, respectively. The tangential stresses increase until their norm reaches the critical value $\nu|\sigma_n|$. Then, sliding occurs in opposite direction to the tangential stresses. All node on the contact boundary lying in between the minimum and maximum of the tangential stresses are sticky nodes, all others are sliding nodes.

REFERENCES

[BBJ+97] P. Bastian, K. Birken, K. Johannsen, S. Lang, N. Neuss, H. Rentz-Reichert, and C. Wieners. UG – a flexible software toolbox for solving partial differential equations. *Computing and Visualization in Science*, 1:27–40, 1997.

[BC84] C. Baiocchi and A. Capelo. *Variational and quasivariational inequalities. Applications to free-boundary value problems.* John Wiley & Sons Ltd., 1984.

[BD98] D. Braess and W. Dahmen. Stability estimates of the mortar finite element method for 3–dimensional problems. *East–West J. Numer. Math.*, 6:249–263, 1998.

[Ben99] F. Ben Belgacem. The mortar finite element method with Lagrange multipliers. *Numer. Math.*, 84:173–197, 1999.

[BGK87] P. Boieri, F. Gastaldi, and D. Kinderlehrer. Existence, uniqueness and regularity results for the two–body contact problem. *Applied Mathematics and Optimzation*, 15:251–227, 1987.

[BHL97] F. Ben Belgacem, P. Hild, and P. Laborde. Approximation of the unilateral contact problem by the mortar finite element method. *C. R. Acad. Sci., Paris, Ser. I*, 324:123–127, 1997.

[BHL99] F. Ben Belgacem, P. Hild, and P. Laborde. Extension of the mortar finite element method to a variational inequality modeling unilateral contact. *Math. Models Methods Appl. Sci.*, 9:287–303, 1999.

[BMP93] C. Bernardi, Y. Maday, and A.T. Patera. Domain decomposition by the mortar element method. In H. Kaper et al., editor, *In: Asymptotic and numerical methods for partial differential equations with critical parameters*, pages 269–286. Reidel, Dordrecht, 1993.

[BMP94] C. Bernardi, Y. Maday, and T. Patera. A new nonconforming approach to domain decomposition: The mortar element method. In H. Brezis and J. L. Lions, editors, *Nonlinear Partial Differential Equations and Their Applications*, pages 13–51. Pitman, 1994.

[CHP00] P. Coorevits, P. Hild, and J.-P. Pelle. A posteriori error estimation for unilateral contact with matching and non-matching meshes. *Comput. Methods Appl. Mech. Eng.*, 186:65–83, 2000.

[CSW99] C. Carstensen, O. Scherf, and P. Wriggers. Adaptive finite elements for elastic bodies in contact. *SIAM J. Sci. Comp.*, 20(5):1605–1626, 1999.

[DNS99] Z. Dostal, F.A.M. Gomes Neto, and S.A. Santos. Solution of contact problems by FETI domain decomposition with natural coarse space projections. *Comp. Meth Appl. Mech. Eng.*, 1999. to appear.

[Dry99] M. Dryja. A Dirichlet–Neumann algorithm for elliptic mortar finite element problems. In W. Hackbusch and S. Sauter, editors, *Numerical Techniques for Composite Materials*, Notes on Numerical Fluid Mechanics. Vieweg, Braunschweig, Submitted to 15th GAMM–Seminar 1999.

[Dry01] M. Dryja. The Dirichlet–Neumann algorithm for mortar saddle point problems. *BIT*, 41, to appear 2001.

[Eck96] C. Eck. *Existenz und Regularität der Lösungen für Kontaktprobleme mit Reibung.* PhD thesis, Math. Inst. A der Universität Stuttgart, 1996.

[EJ98] C. Eck and J. Jarušec. Existence results for the static contact problem with Coulomb friction. *Math. Models Methods Appl. Sci.*, 8:445–468, 1998.

[ESW99] C. Eck, O. Steinbach, and W.L. Wendland. A symmetric boundary element method for

contact problems with friction. *Mathematics and Computers in Simulation*, 50:43–61, 1999.

[GJT81] R. Glowinski, J.L.Lions, and R. Trémolières. *Numerical Analysis of variational inequalities*, volume 8 of *Studies in Mathematics and its applications*. North–Holland, 1981.

[Has92] J. Haslinger. Signorini problem with Coulomb's law of friction. Shape optimization in contact problems. *International J. for numerical methods in engineering*, 34:223–231, 1992.

[Her82] H. Hertz. Über die Berührung fester elastischer Körper. *J.f. Math.*, 92, 1882.

[HH80] J. Haslinger and I. Hlaváček. Contact between elastic bodies. I. continuous problems. *Apl. Mat.*, 25:324–327, 1980.

[HH81] J. Haslinger and I. Hlaváček. Contact between elastic bodies. II. finite element analysis. *Apl. Mat.*, 26:263–290, 1981.

[Hil00] P. Hild. Numerical implementation of two nonconforming finite element methods for unilateral contact. *Comput. Methods Appl. Mech. Eng.*, 184:99–123, 2000.

[IHL88] J. Nečas I. Hlaváček, J. Haslinger and J. Lovíšek. *Solution of variational inequalities in mechanics*. Springer, Berlin, 1988.

[IW92] A. Ibrahimbegovic and E.L. Wilson. Unified computational model for static and dynamic frictional contact. *International J. for numerical methods in engineering*, 34:233–247, 1992.

[KB92] A. KLarbring and G. Björkman. Solution of large displacement contact problems with friction using Newton's method for generalized equations. *International J. for numerical methods in engineering*, 34:249–269, 1992.

[KK99] R. Kornhuber and R. Krause. On monotone multigrid methods for the Signorini problem. In W. Hackbusch and S.A. Sauter, editors, *Numerical Techniques for Composite Materials*, Proceedings of the 15th GAMM Seminar Kiel, 1999. in preparation.

[KK00] R. Kornhuber and R. Krause. Adaptive multigrid methods for Signorini's problem in linear elasticity. to appear, 2000.

[KO88a] N. Kikuchi and J.T. Oden. *Contact Problems in elasticity*. SIAM, Philadelphia, 1988.

[KO88b] N. Kikuchi and J.T. Oden. *Contact problems in elasticity: A study of variational inequalities and finite element methods*. SIAM Studies in Applied Mathematics 8, Philadelphia, 1988.

[Kor97a] R. Kornhuber. *Adaptive monotone multigrid methods for nonlinear variational problems*. Teubner–Verlag, Stuttgart, 1997.

[Kor97b] R. Kornhuber. Adaptive monotone multigrid methods for some non–smooth optimization problems. In R. Glowinski et al., editor, *Domain Decomposition Methods in Sciences and Engeneering*, pages 177–191. Wiley, 1997.

[Kra01] R.H. Krause. *Monotone Multigrid Methods for Signorini's Problem with Friction*. PhD thesis, FU Berlin, 2001.

[NJH80] J. Nečas, J. Jarušec, and J. Haslinger. On the solutionof the variational inequality to the signorini problem with small friction. *Bollettino U.M.I.*, 17:796–811, 1980.

[PC99] G. Pietrzak and A. Curnier. Large deformation frictional contact mechanics: continuum formulation and augmented Lagrangian treatment. *Computer Methods in Applied Mechanics and Engeneering*, 177(3–4):351–381, 1999.

[Tal94] P. Le Tallec. *Handbook of Numerical Analysis*, volume III, chapter Numerical Methods for Nonlinear Three-Dimensional Elasticity. Nort–Holland, 1994. P.G. Ciarlet and J.L. Lions *(Eds.)*.

[WG97] K. Willner and L. Gaul. Contact description by fem based on interface physics. In *Computational Plasticity V*, Barcelona, Spain, 1997.

[Woh00] B.I. Wohlmuth. A mortar finite element method using dual spaces for the Lagrange multiplier. *SINUM*, 38:989–1014, 2000.

[Woh01] B.I. Wohlmuth. *Discretization Methods and Iterative Solvers Based on Domain Decomposition*. Springer Heidelberg, 2001.

[Wri95] P. Wriggers. Finite element algorithms for contact problems. *Arch. Comp. Meth. Engrg.*, 2:1–49, 1995.